Applied Catalysis B: Environmental 89 (2009) 97–103

Contents lists available at ScienceDirect

Applied Catalysis B: Environmental

journal homepage: www.elsevier.com/locate/apcatb

Thermally stable $Pt/K_2Ti_2O_5$ as high-temperature NO_x storage and reduction catalyst

Qiang Wang [a], Ji Hyang Sohn [b], Jong Shik Chung [a,b,*]

[a] School of Environmental Science and Engineering, POSTECH, Pohang 790-784, Republic of Korea
[b] Department of Chemical Engineering, POSTECH, Pohang 790-784, Republic of Korea

ARTICLE INFO

Article history:
Received 12 September 2008
Received in revised form 7 December 2008
Accepted 9 December 2008
Available online 24 December 2008

Keywords:
High temperature
NO_x storage-reduction
$Pt/K_2Ti_2O_5$
Thermal stability
Structure transformation

ABSTRACT

$Pt/K_2Ti_2O_5$ is developed as a high-temperature NO_x storage and reduction (NSR) catalyst. $K_2Ti_2O_5$, in place of alkali metals and γ-Al_2O_3, works as both support and NO_x adsorber; and, unlike alkali-doped NSR catalysts that tend to deactivate at temperature higher than 500 °C, $K_2Ti_2O_5$ shows stable NO_x adsorption in a high temperature range of 500–600 °C. The NO_x storage and reduction performance over $Pt/K_2Ti_2O_5$ is studied by various means, including temperature-programmed adsorption, isothermal storage, and lean–rich cycling experiments. A maximum value of adsorbed NO_x species (close to 1.2 mmol/g catalyst) is achieved at 550 °C. Temperature-programmed de-sorption reveals that the adsorbed NO_x on $Pt/K_2Ti_2O_5$ is highly stable, with a peak at 720 °C. Thermal stability investigations indicate $Pt/K_2Ti_2O_5$ has a much higher stability than $Pt–K/TiO_2$. Mechanism studies reveal that KNO_3-like compound is formed after NO_x adsorption, and that NO_x storage and reduction process on $K_2Ti_2O_5$ is accompanied by a structure transformation between $K_2Ti_2O_5$ and $K_2Ti_6O_{13}$.

1. Introduction

Conventional three-way catalysts (TWCs) are highly efficient in reducing nitrogen oxide (NO_x), CO, and unburned hydrocarbon (HC) emissions from gasoline engines, which work at stoichiometric air/fuel ratio ($A/F = 14.7$) [1,2]; however, the general demand for reduced CO_2 emissions and the requirement of more fuel-efficient gasoline engines has led to the development of lean-burn engines that operate at a significantly higher air/fuel ratio ($A/F > 14.7$) [3–5]. Lean-burn engines run under conditions in which the exhaust gas contains percentage levels of O_2 and the reduction of NO_x emissions on a TWC falls to very low levels. The reduction of NO_x under lean operating conditions is perhaps the greatest challenge in this field [6].

A promising approach for NO_x removal under lean conditions is based on the NO_x storage-reduction (NSR) concept [7,8]. NSR catalytic systems are operated under alternating lean and rich conditions: NO_x is stored on the catalyst under lean conditions and subsequently converted to nitrogen by unburned hydrocarbons under rich conditions. A typical NSR catalyst consists of a high-surface-area support (e.g., γ-Al_2O_3), an NO_x-storage component (alkaline or earth alkaline metal oxide), and a noble metal (e.g., Pt) for both the oxidation of NO and hydrocarbons and the reduction of stored NO_x [9–15]. The most popular and classical NSR catalyst is $Pt–Ba/\gamma$-Al_2O_3, as developed by Toyota [16–18]; however, although many experimental studies have investigated the $Pt–Ba/\gamma$-Al_2O_3 catalyst and theoretical models have been developed for this reaction, catalyst deactivations – especially thermal deterioration and sulfur poisoning – have hindered its commercial application [6,7,19–22].

It is well known that such alkali-doped NSR catalysts are mainly operated within the temperature range of 200–400 °C, as their capacities above 400 °C are limited by the NO_x storage amount [20,23,24]. Therefore, high-temperature (500–600 °C) NO_x abatement technology represents an important challenge. For high-speed motor vehicles with lean-burn gasoline engines, the exhaust temperature can exceed 600 °C [24]. The reactions that occur between NO_x storage compound and support at high temperatures (e.g., $BaO + Al_2O_3 \rightarrow BaAl_2O_4$) mean that there are few reports on high-temperature NSR catalysts. To the best of our knowledge, only Takahashi et al. [24] have reported a catalyst $Pt–K/MgAl_2O_4$ with enhanced NO_x storage capacity at high temperature; however, this remains an alkali-doped NSR catalyst limited by problems with thermal stability and sulfur poisoning.

Although K has superior NO_x storage capacity and TiO_2 is relatively resistant to SO_2 poisoning, the solid reaction between them, which forms potassium titanates, has hindered research into the application of both K and TiO_2 as NSR catalysts [25–27]. Potassium titanates are mainly used as photo-catalyst, ion-

* Corresponding author at: San 31, Hyoja-Dong, Nam-Ku, Pohang 790-784, Republic of Korea. Tel.: +82 54 279 2267; fax: +82 54 279 5528.
E-mail address: jsc@postech.ac.kr (J.S. Chung).

0926-3373/$ – see front matter © 2009 Elsevier B.V. All rights reserved.
doi:10.1016/j.apcatb.2008.12.007

Table 1
Procedures and corresponding testing conditions used in the present work.

Procedures	Testing conditions
Temperature-programmed adsorption	900 ppm NO + 10% O_2 (or 900 ppm NO_2) in He, 200 ml/min, temperature 0–600 °C, 2 °C/min, GHSV 30,000 h^{-1}
Isothermal adsorption	430 ppm NO (or 700 ppm NO_2), 10% O_2 in He, 200 ml/min, temperature 550 °C or 350 °C, GHSV 15,000 h^{-1}
Lean–rich cycling tests	Lean: 400 ppm NO, 5% O_2 in He, 200 ml/min, 5 min per cycle, GHSV 15,000 h^{-1} Rich: 400 ppm NO, 3.5% H_2 in He, 200 ml/min, 1 min per cycle, GHSV 15,000 h^{-1}
Temperature-programmed de-sorption	460 ppm NO, 200 ml/min He, temperature 0–800 °C, 10 °C/min, GHSV 90,000 h^{-1}
Thermal aging	Procedure one: 10% O_2 or 3.5% H_2, 200 ml/min, temperature 700 °C, GHSV 15,000 h^{-1} Procedure two: the gas compositions of lean and rich phases are same to those used in cycling tests, lean 5 min, rich 1 min, 700 °C, 5 h, GHSV 15,000 h^{-1}

exchanger, host materials for intercalation of organic compounds, fuel cell electrolytes, advanced reinforcing materials for brakes and so on; their activities in terms of NO_x storage have yet to be considered in detail [28–33].

Our investigation surprisingly revealed that $K_2Ti_2O_5$ possesses NO_x storage capacity at 500–600 °C; on this basis, we developed a novel high-temperature NSR catalyst, $Pt/K_2Ti_2O_5$. The present work reports on detailed investigations into the synthesis method, structure characterization, activity performance, and mechanism of NO_x storage on $Pt/K_2Ti_2O_5$.

2. Experimental

2.1. Catalyst preparation and characterization

$K_2Ti_2O_5$ was synthesized by a solid state reaction method [34,35]. Briefly, 13.82 g K_2CO_3 (Yakuri Pure Chemical Co., Ltd) and 7.99 g TiO_2 (Hombikat UV 100), and proper amount of water were perfectly mixed by ball milling for 24 h, followed by drying in oven over night. After crushing to fine powders, the sample was calcined at 850 °C for 10 h in air to obtain $K_2Ti_2O_5$. $Pt/K_2Ti_2O_5$ with various Pt loadings (1–4 wt.%) was prepared by incipient wetness impregnation with $H_2PtCl_6{\cdot}5.7H_2O$ (Kojima Chemicals Co., Ltd) as precursor on $K_2Ti_2O_5$ support. The as-prepared samples were dried in an oven overnight and calcined at 850 °C for 10 h. In this work, the Pt loading of $Pt/K_2Ti_2O_5$ is always 2 wt.%, except noted otherwise. For comparison, 2wt.%Pt–20wt.%Ba/γ-Al_2O_3 and 2 wt.% Pt–K/TiO_2 (K/Ti = 0.5 or 1) were also prepared by a procedure similar to previous reports [36,37]. In brief, Pt was first supported on γ-Al_2O_3 (Merck KGaA) or TiO_2 (Hombikat UV 100) by incipient wetness impregnation from $H_2PtCl_6{\cdot}5.7H_2O$ precursor, followed by calcination at 500 °C for 5 h; then Ba or K were added using aqueous solution of barium acetate (Sigma–Aldrich, Inc.) or potassium acetate (Sigma–Aldrich, Inc.) and the obtained samples were further calcined at 500 °C for 5 h.

To evaluate the formations of synthesized $K_2Ti_2O_5$ and $Pt/K_2Ti_2O_5$, and further check their structure changes during NO_x adsorption and reduction, X-ray diffraction patterns were obtained using an X-ray analyzer (XRD, M18XHF, Mac Science Co., Ltd, Yokohama, Japan). Ni-filtered Cu Ka radiation (λ = 1.5415 Å) was used with an X-ray gun operated at 40 kV and 200 mA. Diffraction patterns were obtained within the range of 2θ = 5–70° with a step size of 0.02°. The morphologies of catalysts were investigated by field emission scanning electron microscopy (FE-SEM, Hitachi, S-4200); chemical compositions were determined by energy dispersive X-ray (EDX) analysis. For EDX point analysis, the beam utilized in this work was 100 nm in size; and the corresponding diameter of the analyzing spot was around 1 μm. Fourier transform infrared spectrometer (FT-IR) experiments were performed using a Perkin-Elmer 2000 FT-IR spectrophotometer to check the adsorbed NO_x species. A self-supporting thin disc of 13 mm in diameter was prepared by pressing 1 mg catalyst powder and 14 mg KBr (FT-IR grade, Aldrich Chem. Co.) using a manual hydraulic press. All spectra were measured with 4 cm^{-1} resolution.

2.2. Measurements of catalytic activity and aging

Catalytic tests were performed in a quartz flow reactor (10 mm internal diameter) for which the set-up has been described previously [34,35]. For monitoring the feed compositions and reaction products, an on-line quadrupole mass spectrometer (Balzers Pfeiffer, USA) was used during the lean–rich cycling tests, and an NO_x analyzer (Chemiluminescence NO–NO_2–NO_x analyzer, Model 42C, high level, Thermo Environmental Instruments, Inc.) was used during the temperature-programmed NO_x adsorption and isothermal NO_x adsorption tests. Temperature-programmed NO_x de-sorption (TPD) was utilized to evaluate the stability of the stored NO_x on the catalysts. The catalysts were first exposed to lean conditions in the cycling test (see Table 1) to attain saturated NO_x storages at the optimum temperatures. $Pt/K_2Ti_2O_5$ was placed at 550 °C, while Pt–Ba/γ-Al_2O_3 and $Pt–K/TiO_2$ were placed at 350 °C. The NO_x-saturated catalysts were then heated under the same lean gas flow from room temperature to 800 °C with an increase rate of 10 °C/min; and the NO_x concentration was evaluated by means of the chemiluminescence NO_x analyzer. Since the inlet gas contained 460 ppm NO, the NO_x concentration in excess of 460 ppm was quantified as NO_x desorbed from the catalysts. To assess thermal stability, two thermal aging procedures were used in this study. The first one is aging $Pt/K_2Ti_2O_5$ at 700 °C in oxidative condition (10% O_2) for 70 h or 200 h, or reductive condition (3.5% H_2) for 5 h, then testing by temperature-programmed adsorptions. The second is aging $Pt/K_2Ti_2O_5$ at 700 °C in lean and rich fluctuating conditions for 5 h. The 5 min lean and 1 min rich atmospheres were alternatively switched during the entire thermal aging. After that, its performance was evaluated by a lean–rich cycling test at 550 °C. Table 1 summarizes the procedures and testing conditions used in the present work. For the isothermal NO_x adsorption tests, the difference in the inlet NO and NO_2 concentrations was due to the limitations of our testing system. Although the vehicle emission gases also contain other reductive agents including CO and hydrocarbons, this work only studied the reduction of the adsorbed NO_x with H_2.

3. Results and discussion

3.1. Characterization of catalyst

The XRD patterns of fresh $Pt/K_2Ti_2O_5$ and fresh $K_2Ti_2O_5$ were analyzed and compared in Fig. 1, from which the characteristic

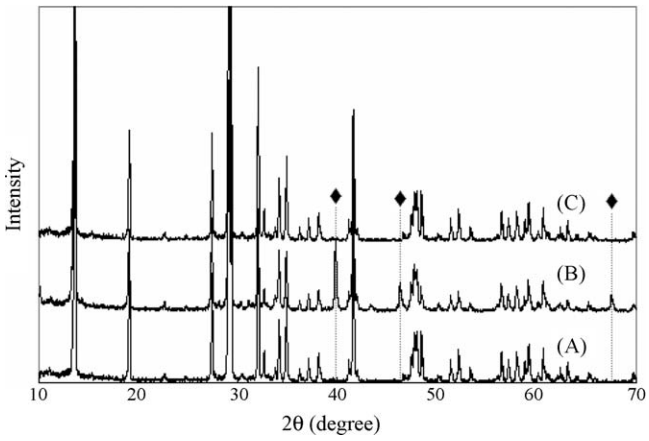

Fig. 1. XRD patterns of (A) fresh $K_2Ti_2O_5$, (B) fresh $Pt/K_2Ti_2O_5$, and (C) reduced $K_2Ti_2O_5$, (◆) Pt.

peaks of Pt are clearly observed at 39.8°, 46.4° and 67.7°, respectively. The other peaks of these two patterns show a close match with each other, indicating that $Pt/K_2Ti_2O_5$ catalyst consisted of Pt loading on $K_2Ti_2O_5$ support. For the conventional alkali-doped NSR catalysts, the NO_x storage compound is normally doped on support; and the reactions between these two compounds (NO_x adsorber and support) are intently to be prevented for a higher NO_x storage capacity. However, in the present work, XRD analyses indicate that potassium has completely reacted with TiO_2 to form a pure $K_2Ti_2O_5$; and no doped potassium species could be found in the synthesized $Pt/K_2Ti_2O_5$. After treatment in a reductive condition (3.5% H_2) at 700 °C for 2 h, the structure of $K_2Ti_2O_5$ kept unchanged (see Fig. 1). It indicates that $K_2Ti_2O_5$ is stable in both oxidative and reductive conditions. The morphology of fresh $Pt/K_2Ti_2O_5$ was investigated by SEM (Fig. 2). Irregular shaped $K_2Ti_2O_5$ particles with size ranging from several micro-meters to several-tenth micro-meters were observed. And the white particles assigned to Pt by EDX analysis are clearly observed on the surface of $K_2Ti_2O_5$ support.

3.2. NO_x adsorption and de-sorption

NO_x storage on fresh $Pt/K_2Ti_2O_5$ was first studied by temperature-programmed adsorptions with NO + O_2. The effluent NO_x

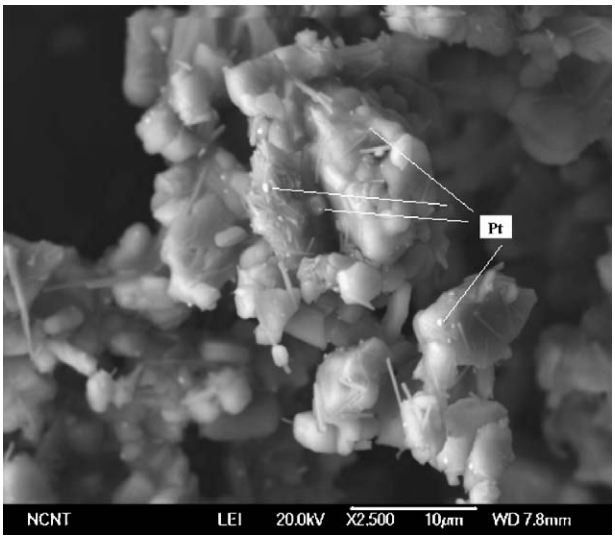

Fig. 2. SEM image of fresh $Pt/K_2Ti_2O_5$.

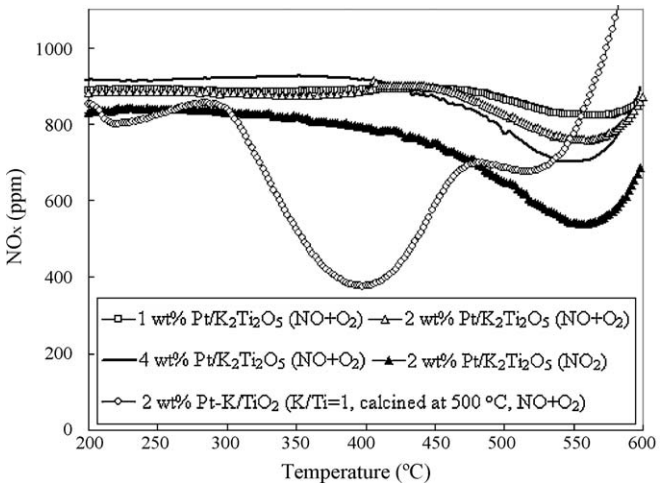

Fig. 3. NO + O_2 or NO_2 adsorptions over fresh 1–4 wt.% $Pt/K_2Ti_2O_5$ and fresh 2 wt.% Pt–K/TiO_2 (K/Ti = 1) during temperature-programmed adsorptions.

concentrations are shown in Fig. 3. Unlike other alkali-doped catalysts, which adsorb NO_x at low temperatures, $Pt/K_2Ti_2O_5$ adsorbed NO_x at high temperatures (500–600 °C). As we disclosed in the following Section 3.5, the mechanism of NO_x storage on $Pt/K_2Ti_2O_5$ could be explained by a structure change from $K_2Ti_2O_5$ to $K_2Ti_6O_{13}$, with the formation of KNO_3-like compound. To initial this reaction, a relatively high temperature is required, which explains the reason why $Pt/K_2Ti_2O_5$ could not store NO_x at low temperature (e.g., <400 °C). For comparison, the temperature-programmed NO + O_2 adsorption on fresh 2 wt.% Pt–K/TiO_2 (K/Ti = 1) was also carried out (Fig. 3). To prevent the reaction between K and TiO_2, a much lower calcination temperature (500 °C) was used for this catalyst. Unlike $Pt/K_2Ti_2O_5$, it adsorbs NO_x in a much wider temperature range (300–550 °C).

The NO_x adsorption rate increased with increasing Pt loading, and was further greatly increased with NO_2 feed compared with NO + O_2 feed. Based on these results, it seems that NO oxidation to NO_2 is the limiting step of NO_x storage for $Pt/K_2Ti_2O_5$. Whereas, for the conventional NSR catalysts, the high-temperature NO_x storage is dependent on not only the NO oxidation, but also the stability of adsorbed NO_x species; since it tends to decompose at high temperature. In the following part, we have proved that the NO_x species adsorbed on $Pt/K_2Ti_2O_5$ is highly stable at 550 °C.

NO_x storage amount on fresh 2 wt.% $Pt/K_2Ti_2O_5$ (0.6 g) was investigated by the isothermal storage of NO + O_2 at 350 °C and 550 °C, respectively, as shown in Fig. 4. As we expected from Fig. 3,

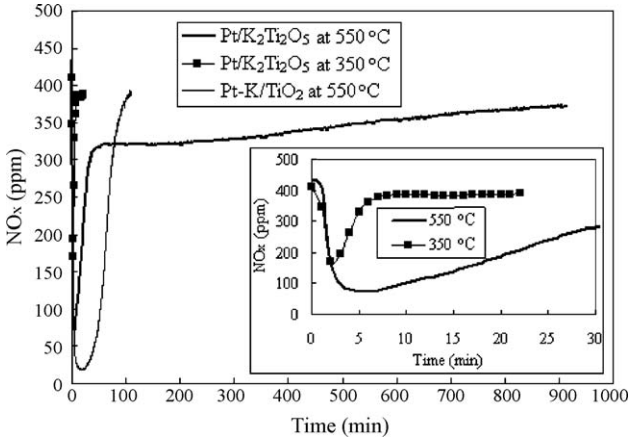

Fig. 4. Isothermal NO_x storages over fresh 2 wt.% $Pt/K_2Ti_2O_5$ at 350 °C or 550 °C, and fresh Pt–K/TiO_2 (K/Ti = 1) at 550 °C.

$Pt/K_2Ti_2O_5$ has negligible NO_x storage at 350 °C. The inset of Fig. 4 clearly shows a rapid saturation of NO_x storage over $Pt/K_2Ti_2O_5$ at 350 °C. However, at high temperature, after switching to lean conditions, the outlet NO_x concentration showed a sharp decrease followed by a gradual increase. The difference between inlet and outlet NO_x concentrations corresponded to the NO_x stored on the catalyst. It took more than 1000 min for $Pt/K_2Ti_2O_5$ to become saturated. Upon calculation, a maximum value of adsorbed NO_x species close to 1.2 mmol/g catalyst was achieved, even higher than that of $Pt–Ba/\gamma\text{-}Al_2O_3$ (0.8 mmol/g) adsorbed at low temperature (350 °C) [38,39]. The consumed potassium corresponds to around 24% of total potassium in $K_2Ti_2O_5$. The isothermal NO_x storage over fresh $Pt–K/TiO_2$ (K/Ti = 1) at 550 °C was also tested, which shows a quite different pattern. The NO_x adsorption rate is very high, and it almost saturated after around 120 min. Its maximum NO_x storage value is only around 0.45 mmol/g, much lower than that of $Pt/K_2Ti_2O_5$ (1.2 mmol/g). At high temperature, the NO_x storage properties are highly dependent on the stability of adsorbed NO_x species and the thermal stability of NO_x storage compounds. For $Pt–Ba/\gamma\text{-}Al_2O_3$ or $Pt–K/TiO_2$, a reaction between Ba (or K) and $\gamma\text{-}Al_2O_3$ (or TiO_2) happens at temperature higher than 550 °C, causing a decreased NO_x storage amount. Consequently, a high temperature is normally intently prevented during operation. However, $Pt/K_2Ti_2O_5$ obtained at 850 °C is much more thermally stable.

Fig. 5 shows the TPD spectra obtained from NO_x-saturated fresh 2wt.%Pt–20wt.%$Ba/\gamma\text{-}Al_2O_3$, 2 wt.% $Pt–K/TiO_2$ (K/Ti = 1) and $Pt/K_2Ti_2O_5$. It is clear that the de-sorption temperature for $Pt/K_2Ti_2O_5$ (T_p = 720 °C) is much higher than those for 2wt.%Pt–20wt.%$Ba/\gamma\text{-}Al_2O_3$ (T_p = 510 °C) and 2 wt.% $Pt–K/TiO_2$ (K/Ti = 1) (640 °C). Basing on our calculation by integrating the profiles, the NO_x de-sorption amount on $Pt/K_2Ti_2O_5$ is around 1.35 times of the value on 2wt.%Pt–20wt.%$Ba/\gamma\text{-}Al_2O_3$. This value is very close to the ratio calculated from the maximum NO_x storage amounts on $Pt/K_2Ti_2O_5$ and 2wt.%Pt–20wt.%$Ba/\gamma\text{-}Al_2O_3$ (1.5). 2 wt.% $Pt–K/TiO_2$ (K/Ti = 1) shows a similar NO_x storage capacity with $Pt/K_2Ti_2O_5$. Takahashi et al. [24] and Park et al. [40] reported even much lower de-sorption temperatures for $Pt–K/\gamma\text{-}Al_2O_3$ (T_p = 380 °C) and $K/\gamma\text{-}Al_2O_3$ (T_p = 400 °C). These data indicate that the stability of the adsorbed NO_x on $Pt/K_2Ti_2O_5$ is much higher than those on alkali-doped NSR catalysts, thereby explaining its high-temperature NO_x storage performance. The essential reason for such enhanced stability is still not clear to us, and further investigation is needed to reveal it. According to the NO_x storage mechanism presented in Section 3.5, the KNO_3-like compound

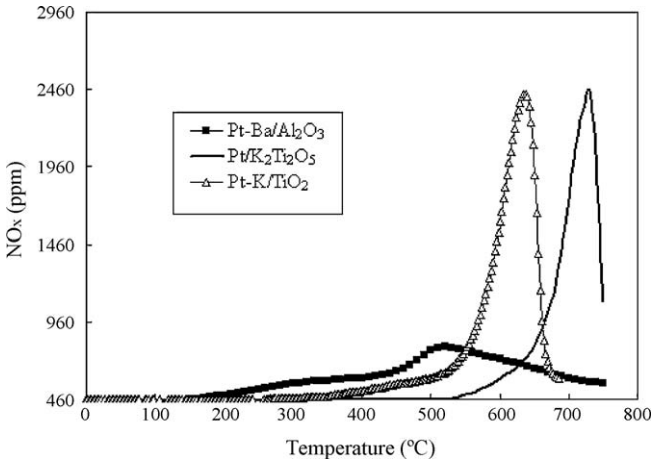

Fig. 5. Evolution of NO_x during temperature-programmed de-sorption of NO_x saturated fresh 2wt.%Pt–20wt.%$Ba/\gamma\text{-}Al_2O_3$, 2 wt.% $Pt–K/TiO_2$ (K/Ti = 1), and 2 wt.% $Pt/K_2Ti_2O_5$.

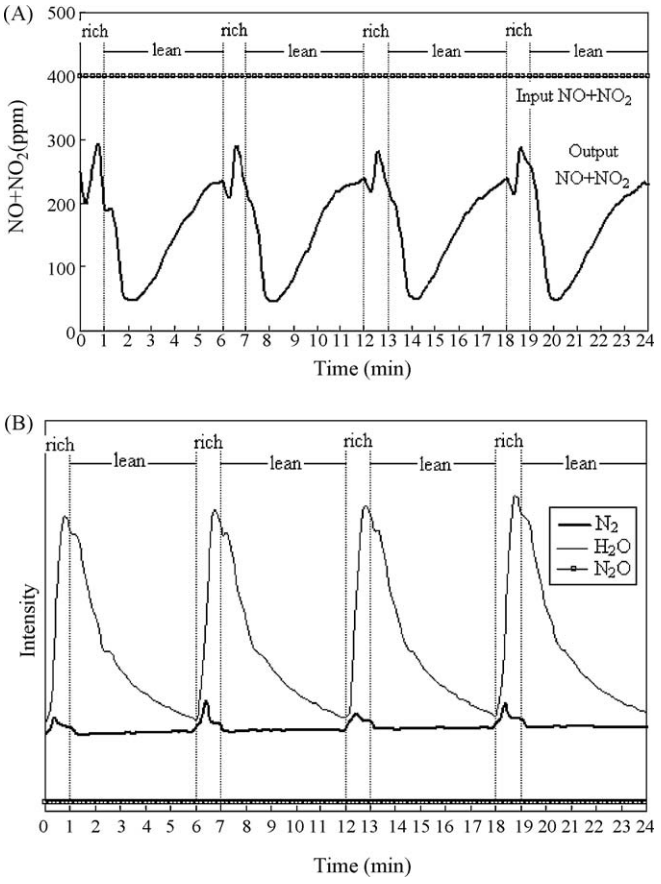

Fig. 6. (A) Evolution of effluent NO + NO_2 during lean–rich cycling test over fresh 2 wt.% $Pt/K_2Ti_2O_5$ at 550 °C. (B) Evolutions of effluent N_2, H_2O and N_2O during lean–rich cycling test over fresh 2 wt.% $Pt/K_2Ti_2O_5$ at 550 °C.

seems formed inside the inter-layers of $Ti_2O_5^{2-}$. The structure of such formed KNO_3-like compound might be different from that on support surface, or it might be trapped by other atoms surrounding.

3.3. Lean–rich cycling test

To further evaluate the reduction activity of adsorbed NO_x, a lean–rich cycling test was carried out over fresh $Pt/K_2Ti_2O_5$ at 550 °C (Fig. 6). During lean periods, NO was first oxidized to NO_2 by Pt; NO_2 was then adsorbed on $K_2Ti_2O_5$ support. During rich periods, the adsorbed NO_x reacted with reducing reagent (H_2) in the presence of Pt. Because of the high reducing activity of Pt, the main products were N_2 and H_2O; almost no N_2O was observed during rich cycles (Fig. 6(B)). Overall, more than 65% of NO_x was removed during the lean–rich cycling tests.

We also investigated the effect of O_2 concentration on the NO_x storage and reduction performance (Fig. 7). When H_2 concentration is low (3.5%), the NO_x storage capacity slightly decreased by increasing O_2 concentration from 4.5% to 10% (see Fig. 7(A)). This might reflect the consumption of H_2 by the slipped O_2 when switching from lean to rich conditions. With higher H_2 concentration (5%), little effect was observed on NO_x removal within the range of 4.5–10% O_2 (see Fig. 7(B)).

3.4. Thermal stability of $Pt/K_2Ti_2O_5$

The thermal stability is a key problem for conventional NSR catalysts, especially for K-doped type. At high temperature, K will

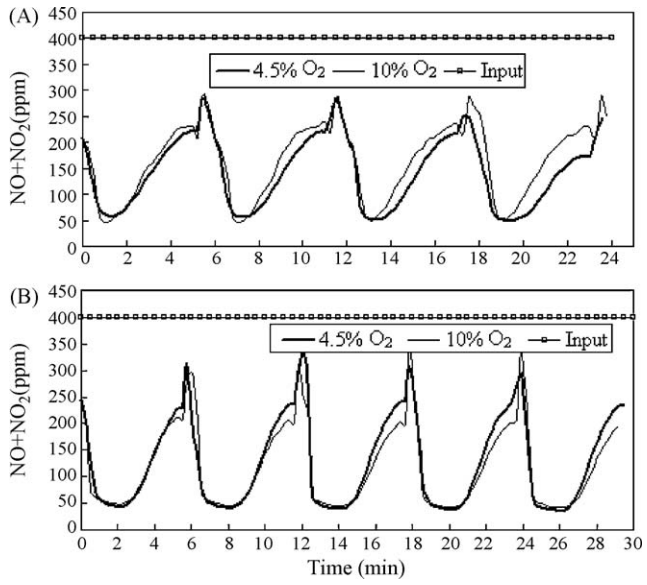

Fig. 7. Effect of O_2 on NO_x storage and reduction during lean–rich cycling tests over fresh 2 wt.% $Pt/K_2Ti_2O_5$ in the present of (A) 3.5% H_2, or (B) 5% H_2.

either react with the support or evaporate. For $Pt/K_2Ti_2O_5$, since K has already reacted with TiO_2 (in form of $K_2Ti_2O_5$), a higher thermal stability is expected. To prove this, $Pt/K_2Ti_2O_5$ was pre-treated in oxidative condition (10% O_2) at 700 °C for 70 h or 200 h. The NO_x storage capacities of fresh and oxidative aged $Pt/K_2Ti_2O_5$ were then evaluated by temperature-programmed adsorptions with NO + O_2. No clear activity loss was observed even after 200 h treatment in the oxidative condition (see Fig. 8), indicating that $Pt/K_2Ti_2O_5$ had high thermal stability. This feature is unique to $Pt/K_2Ti_2O_5$ among all other reported NSR catalysts. Its thermal stability in reductive condition (3.5% H_2) was also evaluated by pre-treating at 700 °C for 5 h. Fig. 8 shows that its NO_x storage activity was even increased after reduction. Since we have proved that $K_2Ti_2O_5$ is structurally stable in reductive condition (see Fig. 1), the enhanced performance of reduced $Pt/K_2Ti_2O_5$ might be due to the reduction of doped Pt. Després et al. [41] has reported that the reduced Pt showed higher NO oxidation activity.

Lean–rich cycling tests over fresh $Pt/K_2Ti_2O_5$ and lean and rich fluctuating aged $Pt/K_2Ti_2O_5$ (denoted as lean–rich aged $Pt/K_2Ti_2O_5$) were also investigated, as shown in Fig. 9. After 4 cycles, the

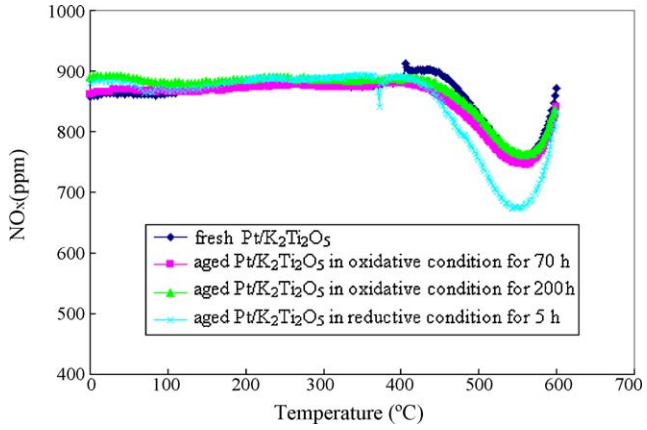

Fig. 8. Temperature-programmed adsorptions of NO + O_2 over fresh $Pt/K_2Ti_2O_5$, oxidizing aged $Pt/K_2Ti_2O_5$ in oxidative condition (10% O_2) at 700 °C for 70 h or 200 h, and reducing aged $Pt/K_2Ti_2O_5$ in reductive condition (3.5% H_2) at 700 °C for 5 h, respectively.

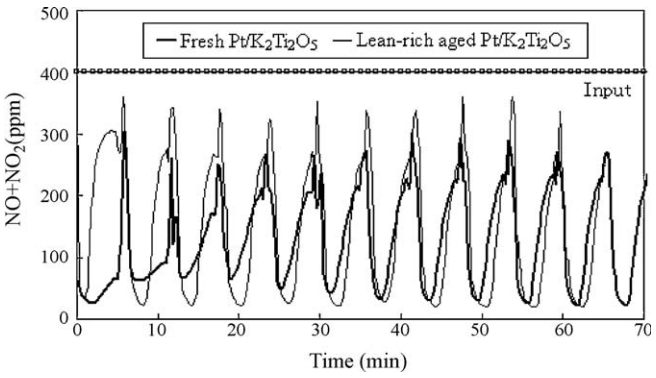

Fig. 9. Evolutions of effluent NO + NO_2 during lean–rich cycling tests over fresh and lean–rich aged $Pt/K_2Ti_2O_5$ at 550 °C.

performance of fresh $Pt/K_2Ti_2O_5$ became stable; and no deactivation occurred within 70 min. Its superior stability was further confirmed by aging the sample in a lean–rich fluctuating condition at 700 °C for 5 h. Comparing to fresh $Pt/K_2Ti_2O_5$, a similar NO_x storage and reduction performance was obtained over the lean–rich aged sample. However, Fig. 10 shows that Pt–K/TiO_2 catalysts have much worse thermal stabilities at 550 °C. The initial performance over both Pt–K/TiO_2 (K/Ti = 0.5) and Pt–K/TiO_2 (K/Ti = 1) was very good; and almost all of the NO_x could be converted to N_2. Nevertheless, their performance decreased rapidly with time, and finally lost most of their activities.

3.5. Adsorption site and mechanism

In addition to catalytic performance, gaining an understanding of the adsorption site is a key issue for NSR catalysts. For conventional NSR catalysts such as Pt–Ba/γ-Al_2O_3 and Pt–K/TiO_2, NO_x is adsorbed on the doped alkali metal oxides as nitrite or nitrate. Since it is widely accepted that K will lose NO_x storage capacity after reacting with TiO_2, people might expect that some K came out from the bulk to surface during the synthesis of $Pt/K_2Ti_2O_5$. To eliminate such a doubt, we demonstrated that fresh $K_2Ti_2O_5$ itself adsorbed NO_2 in the temperature range of 500–600 °C by the temperature-programmed adsorption of NO_2 on pure $K_2Ti_2O_5$, as shown in Fig. 11. Its adsorption capacity was also evaluated by the isothermal storage of 700 ppm NO_2 at 550 °C with 1.5 g $K_2Ti_2O_5$; saturation was obtained after 1750 min. Based on calculations, a maximum value of around 1.4 mmol NO_x per gram of $K_2Ti_2O_5$ was achieved, similar to the value for fresh $Pt/K_2Ti_2O_5$ (1.2 mmol/g).

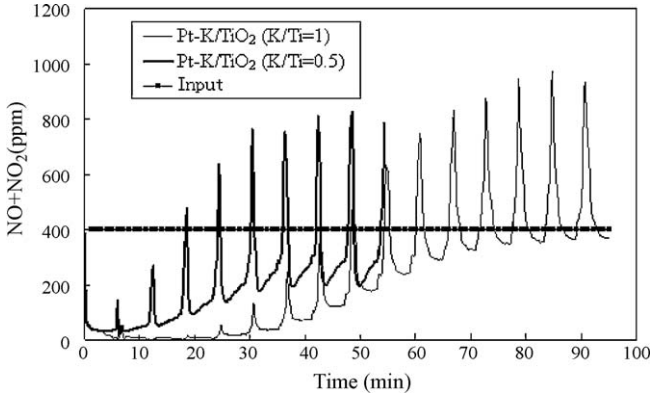

Fig. 10. Evolutions of effluent NO + NO_2 during lean–rich cycling tests over fresh 2 wt.% Pt–K/TiO_2 (K/Ti = 0.5) and 2 wt.% Pt–K/TiO_2 (K/Ti = 1) at 550 °C.

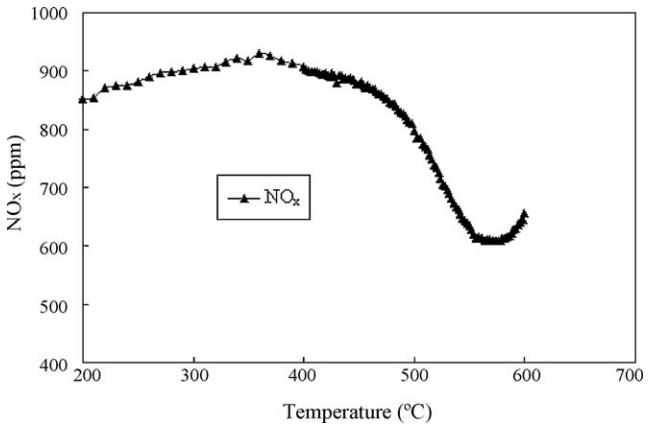

Fig. 11. Temperature-programmed adsorption of NO_2 over fresh pure $K_2Ti_2O_5$.

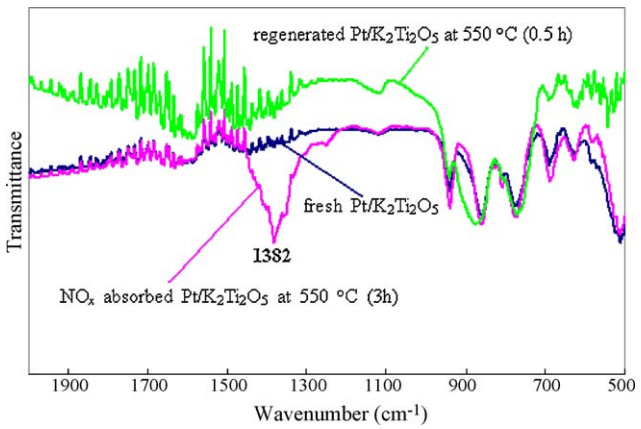

Fig. 13. FTIR of fresh $Pt/K_2Ti_2O_5$, NO_x adsorbed $Pt/K_2Ti_2O_5$ at 550 °C (3 h) and regenerated $Pt/K_2Ti_2O_5$ at 550 °C (0.5 h).

The NO_x adsorption mechanism for $Pt/K_2Ti_2O_5$ is different from that for alkali-doped NSR catalysts, as K had already reacted with TiO_2 to form potassium dititanate. To understand the exact mechanism, fresh $K_2Ti_2O_5$ was first treated with NO_2 at 550 °C for various times; the XRD patterns were then analyzed and compared with that of the fresh sample (Fig. 12). With increasing NO_2 adsorption time, the structure of $K_2Ti_2O_5$ gradually transformed to another potassium titanate, similar to $K_2Ti_6O_{13}$. For NO_2-adsorbed $K_2Ti_2O_5$ (6 h), the peak at 11.5° was much broader than that of synthesized fresh $K_2Ti_6O_{13}$, indicating that the $K_2Ti_6O_{13}$ particles that formed by adsorbing NO_2 on $K_2Ti_2O_5$ were very small.

Peaks at 23.6–23.8°, 29.4°, 32.4°, 33.6–33.8°, 41.1°, and 46.6° gradually appeared, which indicate that KNO_3-like compound (PDF 05-0377) was formed by NO_2 adsorption. The formation of KNO_3-like compound was further confirmed by FT-IR analyses (Fig. 13). A peak at 1382 cm^{-1} appeared after NO_x adsorption, and was assigned as free ionic nitrate [9,34,42,43]. After regenerating the sample at 550 °C with 3.5% H_2 for 0.5 h, the nitrate peak at 1382 cm^{-1} disappeared, and its FT-IR pattern was exactly the same as that for fresh $Pt/K_2Ti_2O_5$, indicating that the adsorbed NO_x was reduced by H_2.

Fig. 14 shows that the NO_2-adsorbed $K_2Ti_2O_5$ could be regenerated by 3.5% H_2 during temperature-programmed ramping (25–750 °C). After regeneration, the structure transformed back to $K_2Ti_2O_5$, indicating that the structure transformation is reversible. All the analyses indicate that NO_2 was adsorbed on the K sites located in the inter-layers of $K_2Ti_2O_5$, thereby consuming a certain amount of potassium. The resulting shortage of potassium meant that $K_2Ti_2O_5$ transformed to other titanates with lower K/Ti values, such as $K_2Ti_6O_{13}$. The NO_x storage and reduction performances over $Pt/K_2Ti_2O_5$ were achieved by a reversible structure transformation between $K_2Ti_2O_5$ and $K_2Ti_6O_{13}$.

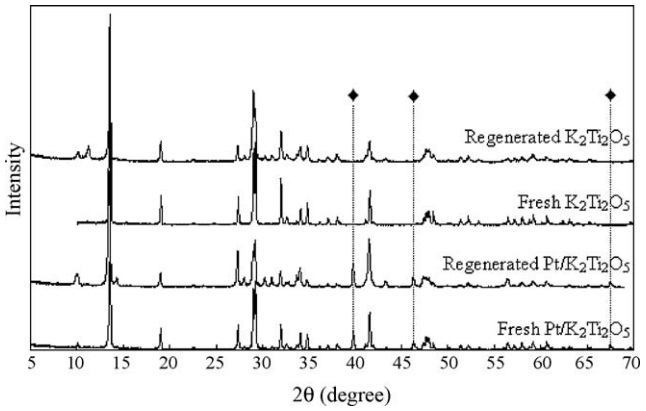

Fig. 14. XRD patterns of fresh $K_2Ti_2O_5$ and $Pt/K_2Ti_2O_5$, and regenerated $K_2Ti_2O_5$ and $Pt/K_2Ti_2O_5$, (◆) Pt.

The NO_x storage and reduction mechanism over $Pt/K_2Ti_2O_5$ during lean and rich conditions was proposed as Fig. 15. During lean period, NO is first oxidized to NO_2, and NO_2 is then adsorbed on K to form KNO_3-like compound. This process is accompanied by a structure change from $K_2Ti_2O_5$ to $K_2Ti_6O_{13}$. During rich period,

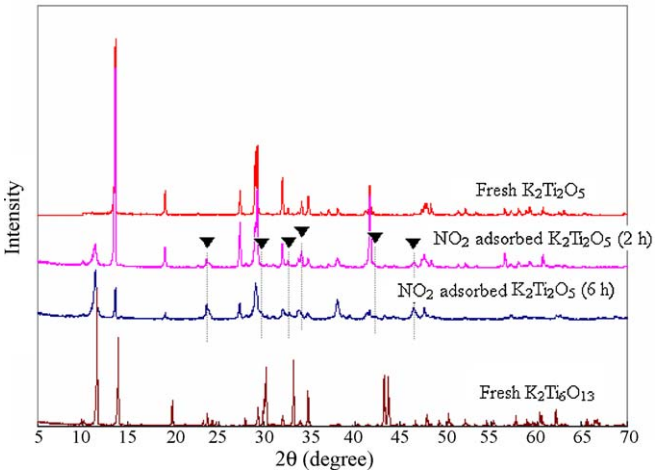

Fig. 12. XRD patterns of fresh $K_2Ti_2O_5$, NO_2 adsorbed $K_2Ti_2O_5$ (2 h), NO_2 adsorbed $K_2Ti_2O_5$ (6 h), and fresh $K_2Ti_6O_{13}$; (▼) KNO_3 (PDF 05-0377).

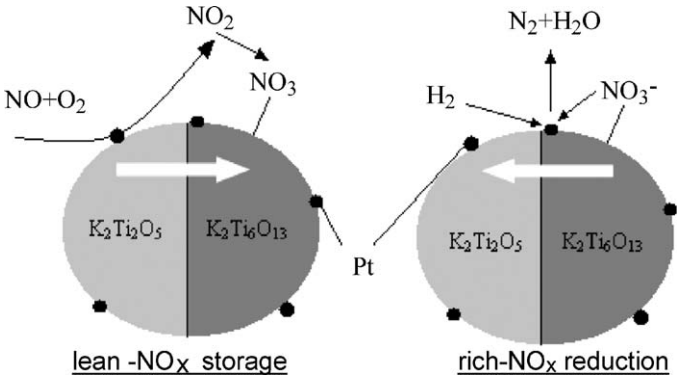

Fig. 15. Proposed NO_x storage and reduction mechanism over $Pt/K_2Ti_2O_5$ in lean and rich conditions.

the adsorbed NO_x species will release and react with reductive agent (H_2) in the presence Pt, forming N_2 and H_2O. In the mean time, $K_2Ti_6O_{13}$ transforms back to $K_2Ti_2O_5$ by reacting with the released K.

4. Conclusions

In the present work, $K_2Ti_2O_5$, prepared by solid state reaction between TiO_2 and K, showed NO_x adsorption activity at 500–600 °C; on this basis, $Pt/K_2Ti_2O_5$ obtained by impregnating Pt on $K_2Ti_2O_5$ was further developed as a high-temperature NSR catalyst. Here, $K_2Ti_2O_5$ worked as both support and NO_x absorber. XRD and SEM–EDX analyses indicated that K has completely reacted with TiO_2 to form $K_2Ti_2O_5$, and no doped K was found in the synthesized samples. The effects of Pt loadings and NO_x species were studied by temperature-programmed adsorptions, revealing that the oxidation of NO to NO_2 is a limiting step of NO_x storage for $Pt/K_2Ti_2O_5$ at high temperatures. TPD results demonstrated high stability ($T_p \sim 720$ °C) of NO_x adsorbed on $Pt/K_2Ti_2O_5$. A maximum value of adsorbed NO_x close to 1.2 mmol/g catalyst was obtained by isothermal storage at 550 °C, even higher than that of Pt–Ba/γ-Al_2O_3 (0.8 mmol/g, 350 °C). Lean–rich cycling tests performed at 550 °C revealed that the adsorbed NO_x is easily reduced to N_2 and H_2O by reducing agents (e.g., H_2); almost no N_2O was observed during rich conditions. Lean–rich cycling operations over fresh and aged $Pt/K_2Ti_2O_5$ at 550 °C revealed its superior thermal stability; nevertheless, Pt–K/TiO_2 showed a much worse stability and deactivated rapidly in the same conditions. XRD and FT-IR analyses revealed that KNO_3-like compound formed after NO_2 adsorption on $K_2Ti_2O_5$; consumption of K meant that $K_2Ti_2O_5$ transformed to other types of potassium titanate (most likely $K_2Ti_6O_{13}$). After regenerating the NO_x-adsorbed $K_2Ti_2O_5$ by H_2 during temperature-programmed ramping (25–750 °C), the sample transformed back to $K_2Ti_2O_5$, indicating that the structure transformation is reversible. Considering its high NO_x storage capacity and good thermal stability, $Pt/K_2Ti_2O_5$ is potential for practical application as a high-temperature NSR catalyst.

Acknowledgements

The financial support from Korea Institute of Science and Technology Evaluation and Planning (KISTEP, M1-0214-00-0133), Korea Science and Engineering Foundation (KOSEF, M02-2004-000-10512-0), and the BK21 program of Korea is gratefully acknowledged by authors.

References

[1] B.H. Engler, D. Lindner, E.S. Lox, A.S. Sindlinger, K. Ostgathe, Stud. Surf. Sci. Catal. 96 (1995) 441–460.
[2] J.G. Nunan, H.J. Robota, M.J. Cohn, S.A. Bradley, J. Catal. 133 (1992) 309–324.
[3] R.D. Clayton, M.P. Harold, V. Balakotaiah, Appl. Catal. B: Environ. 84 (2008) 616–630.
[4] L. Li, J. Chen, S. Zhang, F. Zhang, N. Guan, T. Wang, S. Liu, Environ. Sci. Technol. 39 (2005) 2841–2847.
[5] H.Y. Huang, R.Q. Long, R.T. Yang, Energy Fuel 15 (2001) 205–213.
[6] F. Basile, G. Fornasari, A. Grimandi, M. Livi, A. Vaccari, Appl. Catal. B: Environ. 69 (2006) 58–64.
[7] N. Takahashi, H. Shinjoh, T. Iijima, T. Suzuki, K. Yamazaki, K. Yokota, H. Suzuki, N. Miyoshi, S. Matsumoto, T. Tanizawa, T. Tanaka, S. Tateishi, K. Kasahara, Catal. Today 27 (1996) 63–69.
[8] S. Matsumoto, Catal. Today 29 (1996) 43–45.
[9] I. Nova, L. Castoldi, L. Lietti, E. Tronconi, P. Forzatti, F. Prinetto, G. Ghiotti, J. Catal. 222 (2004) 377–388.
[10] H. Imagawa, T. Tanaka, N. Takahashi, S. Matsunaga, A. Suda, H. Shinjoh, Appl. Catal. B: Environ. 86 (2009) 63–68.
[11] J. Szanyi, J.H. Kwak, D.H. Kim, X. Wang, R. Chimentao, J. Hanson, W.S. Epling, C.H.F. Peden, J. Phys. Chem. C 111 (2007) 4678–4687.
[12] M. Piacentini, M. Maciejewski, A. Baiker, Appl. Catal. B: Environ. 72 (2007) 105–117.
[13] W.S. Epling, A. Yezerets, N.W. Currier, Appl. Catal. B: Environ. 74 (2007) 117–129.
[14] I. Malpartida, M.A.L. Vargas, L.J. Alemany, E. Finocchio, G. Busca, Appl. Catal. B: Environ. 80 (2008) 214–225.
[15] T. Lesage, J. Saussey, S. Malo, M. Hervieu, C. Hedouin, G. Blanchard, M. Daturi, Appl. Catal. B: Environ. 72 (2007) 166–177.
[16] S. Matsumoto, Y. Ikeda, H. Suzuki, M. Ogai, N. Miyoshi, Appl. Catal. B: Environ. 25 (2000) 115–124.
[17] K. Yamazaki, T. Suzuki, N. Takahashi, K. Yokota, M. Sugiura, Appl. Catal. B: Environ. 30 (2001) 459–468.
[18] H. Hirata, I. Hachisuka, Y. Ikeda, S. Tsuji, S. Matsumoto, Top. Catal. 16/17 (2001) 145–149.
[19] L. Lietti, P. Forzatti, I. Nova, E. Tronconi, J. Catal. 204 (2001) 175–191.
[20] M. Takeuchi, S. Matsumoto, Top. Catal. 28 (2004) 151–156.
[21] Y. Su, M.D. Amiridis, Catal. Today 96 (2004) 31–41.
[22] Y. Sakamoto, T. Motohiro, S. Matsunaga, K. Okumura, T. Kayama, K. Yamazaki, T. Tanaka, Y. Kizaki, N. Takahashi, H. Shinjoh, Catal. Today 121 (2007) 217–225.
[23] N. Takahashi, K. Yamazaki, H. Sobukawa, H. Shinjoh, Appl. Catal. B: Environ. 70 (2007) 198–204.
[24] N. Takahashi, S. Matsunaga, T. Tanaka, H. Sobukawa, H. Shinjoh, Appl. Catal. B: Environ. 77 (2007) 73–78.
[25] L.J. Gill, P.G. Blakeman, M.V. Twigg, A.P. Walter, Top. Catal. 28 (2004) 157–164.
[26] J.S. Hepburn, E. Thanasiu, D.A. Dobson, W.L. Watkins, SAE (1996) 962051.
[27] I. Hachisuka, T. Yoshida, H. Ueno, N. Takahashi, A. Suda, M. Sugiura, SAE (2002), 2002-01-0732.
[28] R.B. Yahya, H. Hayashi, T. Nagase, T. Ebina, Y. Onodera, N. Saitoh, Chem. Mater. 13 (2001) 842–847.
[29] N. Bao, X. Feng, Z. Yang, L. Shen, X. Lu, Environ. Sci. Technol. 38 (2004) 2729–2736.
[30] S. Yin, T. Sato, Ind. Eng. Chem. Res. 39 (2000) 4526–4530.
[31] D.J.D. Corcoran, D.P. Tunstall, J.T.S. Irvine, Solid State Ion 136/137 (2000) 297–303.
[32] T. Sasaki, F. Izumi, M. Watanabe, Chem. Mater. 8 (1996) 777–782.
[33] Y.C. Kim, M.H. Cho, S.J. Kim, H. Jang, Wear 264 (2008) 204–210.
[34] Q. Wang, S.Y. Park, J.S. Choi, J.S. Chung, Appl. Catal. B: Environ. 79 (2008) 101–107.
[35] Q. Wang, S.Y. Park, L. Duan, J.S. Chung, Appl. Catal. B: Environ. 85 (2008) 10–16.
[36] M. Casapu, J.D. Grunwaldt, M. Maciejewski, F. Krumeich, A. Baiker, M. Wittrock, S. Eckhoff, Appl. Catal. B: Environ. 78 (2008) 288–300.
[37] S. Hammache, L.R. Evans, E.N. Coker, J.E. Miller, Appl. Catal. B: Environ. 78 (2008) 315–323.
[38] H. Mahzoul, J.F. Brilhac, P. Gilot, Appl. Catal. B: Environ. 20 (1999) 47–55.
[39] L. Castoldi, I. Nova, L. Lietti, P. Forzatti, Catal. Today 96 (2004) 43–52.
[40] S.M. Park, J.W. Park, H.P. Ha, H.S. Han, G. Seo, J. Mol. Catal. A: Chem. 273 (2007) 64–72.
[41] J. Després, M. Elsener, M. Koebel, O. Kröcher, B. Schnyder, A. Wokaun, Appl. Catal. B: Environ. 50 (2004) 73–82.
[42] T.J. Toops, W.S. Epling, J.E. Parks, W.P. Partidge, Appl. Catal. B: Environ. 58 (2005) 255–264.
[43] F. Prinetto, G. Ghiotti, I. Nova, L. Lietti, E. Tronconi, P. Forzatti, J. Phys. Chem. B 105 (2001) 12732–12745.